

**Mutations in the 'DRY' motif of the CB<sub>1</sub> cannabinoid receptor result in biased  
receptor variants**

**Pál Gyombolai<sup>1,2</sup>, András D. Tóth<sup>1</sup>, Dániel Tímár<sup>1</sup>, Gábor Turu<sup>1</sup>, László  
Hunyady<sup>1,2,#</sup>**

<sup>1</sup>Department of Physiology, Faculty of Medicine, Semmelweis University, Budapest,  
Hungary, [gyombolai.pal@med.semmelweis-univ.hu](mailto:gyombolai.pal@med.semmelweis-univ.hu), [toth.andras1@med.semmelweis-univ.hu](mailto:toth.andras1@med.semmelweis-univ.hu), [timar.daniel.sote@gmail.com](mailto:timar.daniel.sote@gmail.com), [туру.gabor@med.semmelweis-univ.hu](mailto:туру.gabor@med.semmelweis-univ.hu)

<sup>2</sup>MTA-SE Laboratory of Molecular Physiology, Hungarian Academy of Sciences and  
Semmelweis University, Budapest, Hungary

<sup>#</sup>Address correspondence to: Prof. Dr. László Hunyady, Department of Physiology, Faculty  
of Medicine, Semmelweis University, H-1444 Budapest, P. O. Box 259, Hungary, Fax: 36-  
1-266-6504, Phone: 36-1-266-9180, E-mail: [Hunyady@puskin.sote.hu](mailto:Hunyady@puskin.sote.hu)

**Short title:** Mutations in the 'DRY' motif of CB<sub>1</sub> receptor

**Keywords:** G proteins, Signal transduction, Mutations, Receptors

**Word count:** 5456

## Abstract

The role of the highly-conserved 'DRY' motif in the signaling of the CB<sub>1</sub> cannabinoid receptor (CB<sub>1</sub>R) was investigated by introducing single, double and triple alanine mutations into this site of the receptor. We found that the CB<sub>1</sub>R-R3.50A mutant displays a partial decrease in its ability to activate heterotrimeric G<sub>o</sub> proteins (~80% of wild-type CB<sub>1</sub>R (CB<sub>1</sub>R-WT)). Moreover, this mutant showed an enhanced basal  $\beta$ -arrestin2 recruitment. More strikingly, the double mutant CB<sub>1</sub>R-D3.49A/R3.50A was biased toward  $\beta$ -arrestins, as it gained a robustly increased  $\beta$ -arrestin1 and  $\beta$ -arrestin2 recruitment ability compared to the wild-type receptor, while its G protein activation was decreased. In contrast, the double mutant CB<sub>1</sub>R-R3.50A/Y3.51A proved to be G protein-biased, as it was practically unable to recruit  $\beta$ -arrestins in response to agonist stimulus, while still activating G proteins, although at a reduced level (~70% of CB<sub>1</sub>R-WT). Agonist-induced ERK1/2 activation of the CB<sub>1</sub>R mutants showed good correlation with their  $\beta$ -arrestin recruitment ability but not with their G protein activation or inhibition of cAMP accumulation. Our results suggest that G protein activation and  $\beta$ -arrestin binding of the CB<sub>1</sub>R are mediated by distinct receptor conformations and the conserved 'DRY' motif plays different roles in the stabilization of these conformations, thus mediating both G protein- and  $\beta$ -arrestin-mediated functions of CB<sub>1</sub>R.

## 1. Introduction

Seven transmembrane receptors (7TMRs) constitute the largest family of plasma membrane receptors. Most of their intracellular effects are mediated via direct coupling to heterotrimeric G proteins. To understand the molecular details of 7TMR activation and G protein coupling, identification of key structural elements regulating these processes is critically important. Using mutational analyses as well as recent high resolution X-ray crystal structure data, such structural features have been extensively mapped (Venkatakrishnan et al. 2013). Among these, the conserved Asp-Arg-Tyr (DRY) motif, located at the beginning of the second intracellular loop (ICL2), seems to play a central role both in the activation and the G protein coupling of class A (rhodopsin-like) 7TMRs (Rasmussen et al. 2011). Nevertheless, the exact nature of this regulatory role is still not completely understood. For instance, although the Arg residue (R3.50) is suggested to directly interact with the G protein  $\alpha$  subunit in the active 7TMR conformation, its non-conservative mutations in many cases fail to impair G protein coupling of the receptor (Fanelli et al. 1999; Rhee et al. 2000; Rovati et al. 2007). Furthermore, Asp (D3.49) is believed to stabilize inactive receptor conformation by forming a salt-bridge with the neighboring R3.50 (Scheer et al. 1996; Scheer et al. 1997; Ballesteros et al. 1998; Ballesteros et al. 2001; Li et al. 2001), however, its mutations can also result in completely diverse phenotypes, depending on the investigated receptor (Rovati et al. 2007). Therefore, the exact role of the DRY motif obviously shows receptor-specific differences, and its detailed analysis for a particular 7TMR seems reasonable.

Besides G proteins,  $\beta$ -arrestins are also able to directly bind to the intracellular surface of an activated 7TMR, leading to the desensitization and internalization of the receptor (Shenoy and Lefkowitz 2011). Moreover, receptor-bound  $\beta$ -arrestins can also serve as a starting point for G protein-independent signaling pathways, such as the activation of the p42/44 mitogen-activated protein kinase (MAP kinase) cascade or Src kinases (Wei et al. 2003; DeWire et al. 2007).

Many data suggest that the  $\beta$ -arrestin-bound conformation of 7TMRs may differ from the one mediating their G protein activation, a fact being implicitly exploited by several functionally selective 7TMR ligands as well as by functionally selective 7TMR mutants, which are able to induce  $\beta$ -arrestin recruitment without affecting G protein coupling or vice versa (Reiter et al. 2012). However, in the lack of a high resolution crystal structure describing a 7TMR in its  $\beta$ -arrestin-bound form, relatively little is known about the receptor-arrestin binding interface. According to the prevailing idea, arrestins utilize two distinct sites to bind to 7TMRs, one of which is a 'phosphorylation sensor', recognizing Ser/Thr-phosphorylated C-terminus of the receptor (Gurevich and Benovic 1993; Gurevich and Gurevich 2006). The other site is a so-called 'activation sensor', which recognizes the active 7TMR conformation, independently of receptor phosphorylation (Gurevich and Gurevich 2006). The 7TMR elements constituting the docking site for the arrestin 'activation sensor' are less understood. The second intracellular loop (ICL2), beginning with the DRY motif, has been proposed to play such a role (Huttenrauch et al. 2002; Marion et al. 2006). Furthermore, complementary roles for the DRY motif and receptor C-terminus in the regulation of  $\beta$ -arrestin binding have been described (Kim and Caron 2008). In addition, mutations of R3.50 in many cases results in basal  $\beta$ -arrestin

86 binding and subsequent constitutively desensitized phenotype of 7TMRs (Barak et al.  
87 2001; Wilbanks et al. 2002). Thus, the conserved DRY motif seems to be involved not  
88 only in G protein coupling, but also in  $\beta$ -arrestin binding of 7TMRs.

89 The CB<sub>1</sub> cannabinoid receptor (CB<sub>1</sub>R) belongs to the 7TMR superfamily. The signaling  
90 pathways originating from CB<sub>1</sub>R are mediated mainly via heterotrimeric G<sub>i/o</sub> proteins,  
91 and include inhibition of cAMP production, activation of GIRK potassium channels,  
92 inhibition of Ca<sub>v</sub> calcium channels, and activation of MAP kinase cascades (Turu and  
93 Hunyady 2010). Moreover, CB<sub>1</sub>R shows basal G protein activation and constitutive  
94 internalization under diverse cellular conditions (Leterrier et al. 2006; McDonald et al.  
95 2007; Turu et al. 2007). Like most other 7TMRs, CB<sub>1</sub>R also recruits  $\beta$ -arrestin following  
96 activation, which leads to the desensitization and internalization of the receptor  
97 (Kouznetsova et al. 2002; Daigle et al. 2008; Gyombolai et al. 2013). The binding  
98 between  $\beta$ -arrestins and CB<sub>1</sub>R is relatively weak, and the affinity of the receptor for  $\beta$ -  
99 arrestin2 ( $\beta$ -arr2) is substantially higher than that for  $\beta$ -arrestin1 ( $\beta$ -arr1) (Gyombolai et  
100 al. 2013). Furthermore,  $\beta$ -arr1 recruitment of CB<sub>1</sub>R appears to be agonist-dependent  
101 (Laprairie et al., 2014; Flores-Otero et al., 2014). Interestingly, in addition to canonical G  
102 protein-mediated intracellular effects, recent data suggest the existence of  $\beta$ -arrestin-  
103 mediated, G protein-independent signaling of CB<sub>1</sub>R, i.e. the p42/44 MAPK (ERK1/2)  
104 activation of the receptor seems to be at least partly mediated by  $\beta$ -arrestins (Ahn et al.  
105 2013a; Mahavadi et al. 2014).

106 Via these cellular events, CB<sub>1</sub>R is involved in the regulation of many important  
107 physiological and pathophysiological processes, such as memory, learning, pain  
108 sensation, metabolic regulation, or the regulation of vascular tone (Pacher et al. 2006).

Moreover, several natural and synthetic cannabinoid ligands are known to stabilize distinct active CB<sub>1</sub>R conformations, i.e. prove to be functionally selective (Glass and Northup 1999; Mukhopadhyay and Howlett 2001; Ahn et al. 2013a). Thus, investigation of the structural elements responsible for G protein- and  $\beta$ -arrestin-mediated CB<sub>1</sub>R functions has a major physiological and pharmacological impact. Accordingly, a number of studies have aimed to identify such regulatory motifs of CB<sub>1</sub>R. A detailed computational model based on the crystal structure of the  $\beta_2$ -adrenergic receptor-G $\alpha_s$  complex, combined with mutational data, suggested that distinct residues in the ICL2 and ICL3 regions of the CB<sub>1</sub>R may be involved in the stabilization of the active, G $\alpha_i$ -coupled receptor conformation (Shim et al. 2013). Two other recent studies analyzed the role of several intramolecular salt-bridges, which may stabilize inactive, partially active and fully active CB<sub>1</sub>R conformations (Ahn et al. 2013b; Scott et al. 2013). According to this model, D3.49 and R3.50 residues form salt-bridges with K4.41 and D6.30, respectively, which (together with a D2.63+K3.28 salt-bridge) may keep the receptor in a partially active conformation under basal conditions.

Less is known about the structural features governing the  $\beta$ -arrestin binding of CB<sub>1</sub>R. The C-terminal Ser/Thr phosphorylation of the receptor seems to play a role, since alanine mutations of these residues impaired agonist-induced  $\beta$ -arrestin recruitment and subsequent internalization of CB<sub>1</sub>R (Daigle et al. 2008).

Although the above studies clearly provide important insights into the molecular details of CB<sub>1</sub>R function, none of them assessed the role of the DRY motif in CB<sub>1</sub>R function directly, i.e. through mutational analysis. More importantly, none of the available studies have aimed to identify  $\beta$ -arrestin-regulatory motifs of CB<sub>1</sub>R other than the receptor C-

terminus. Therefore, our goal was to analyze the role of the conserved DRY sequence in the G protein activation and  $\beta$ -arrestin binding of CB<sub>1</sub>R. We introduced single, double and triple alanine mutations into this site of CB<sub>1</sub>R and applied functional assays directly measuring G protein activation,  $\beta$ -arr2 recruitment and intracellular signaling of wild-type and mutant CB<sub>1</sub>R variants.

## **2. Materials and Methods**

### *2.1. Materials*

The cDNA of the rat vascular CB<sub>1</sub>R was provided by Zsolt Lenkei (Centre National de la Recherche Scientifique, Paris). cDNAs of human  $\beta_1$  and  $\gamma_{11}$  G protein subunits were purchased from the Missouri S&T cDNA Resource Center (Rolla, MO).  $\beta$ -arr2-eGFP cDNA was kindly provided by Dr. Marc G. Caron (Duke University, Durham, NC). Molecular biology enzymes were obtained from Fermentas (Vilnius, Lithuania) and Stratagene (La Jolla, CA). Fetal bovine serum (FBS), OptiMEM, Lipofectamine 2000, and PBS-EDTA were from Invitrogen (Carlsbad, CA). CHO-K1 and HeLa cell lines were obtained from ATCC (American Type Culture Collection, Manassas, VA). Coelenterazine h was from Regis Technologies (Morton Grove, IL). WIN55,212-2, 2-arachydonoylglycerol and AM251 were from Tocris (Bristol, UK). Cell culture dishes and plates for BRET measurements were from Greiner (Kremsmunster, Austria). Anti-pERK1/2, anti-ERK1/2 and HRP-conjugated anti-rabbit and anti-mouse antibodies were

from Cell Signaling Technology Inc. (Beverly, MA). Unless otherwise stated, all other chemicals and reagents were from Sigma (St. Louis, MO).

## *2.2. Plasmid constructs and site-directed mutagenesis*

The mVenus-tagged rat CB<sub>1</sub>R (CB<sub>1</sub>R-mVenus) was created by exchanging the sequence of eYFP in CB<sub>1</sub>R-eYFP (kindly provided by Zsolt Lenkei (Centre National de la Recherche Scientifique, Paris)) to the sequence of mVenus using AgeI and NotI restriction enzymes.  $\alpha_0$ -Rluc and YFP- $\beta_1$  constructs were created from  $\alpha_{0A}$ -CFP (kindly provided by Dr. N. Gautam (Azpiazu and Gautam 2004)), and  $\beta_1$ , respectively, as described previously (Turu et al. 2007).  $\beta$ -arr2-Rluc was constructed as described previously (Turu et al. 2006). Plasma membrane-targeted mVenus (MP-mVenus) was constructed as described previously (Varnai et al. 2007). Plasma membrane-targeted super Renilla luciferase (MP-Sluc) was generated from MP-mVenus by replacing the mVenus coding sequence with the cDNA of super Renilla luciferase (Woo and von Arnim, 2008). The EPAC-based BRET sensor was constructed as described previously (Erdelyi et al. 2014). Mutations in the DRY motif of CB<sub>1</sub>R or CB<sub>1</sub>R-mVenus were inserted by the QuikChange® site-directed mutagenesis kit (Stratagene, La Jolla, CA) according to manufacturer's suggestions. Sequences of all constructs were verified using automated DNA sequencing.

## *2.3. Cell culture and transfection*



CHO or HeLa cells (passage numbers 5 to 15) were maintained in Ham's F12 or DMEM, respectively, supplemented with 10% FBS, (Invitrogen, Carlsbad, CA), 100 µg/ml streptomycin, and 100 IU/ml penicillin in 5% CO<sub>2</sub> at 37 °C. For confocal microscopy experiments, cells were grown on glass coverslips in 6-well plates and transfected with the indicated constructs using Lipofectamine 2000 in OptiMEM following the manufacturer's instructions. For BRET and Western blot experiments, cells were grown on 6-well plates and transfected with the indicated constructs using Lipofectamine 2000 in OptiMEM following the manufacturer's instructions.

#### *2.4. Bioluminescence resonance energy transfer (BRET) measurements*

A detailed description of the BRET measurements applied here can be found in Supplementary Methods.

#### *2.5. Confocal laser-scanning microscopy*

Cells were grown on glass coverslips and transfected with the appropriate constructs (using 2 µg/well CB<sub>1</sub>R-mVenus or 0.5 µg/well β-arr2-GFP and 2 µg/well CB<sub>1</sub>R). Cells were analyzed 22-26 hours later in a modified Krebs-Ringer buffer (see above), using a Zeiss LSM 710 confocal laser scanning microscope.

#### *2.6. Western blot analysis*

A detailed description of the Western blot measurements applied here can be found in Supplementary Methods.

### 2.7. Data analysis

Dose-response curves for G protein,  $\beta$ -arrestin and EPAC BRET measurements were fitted and statistically compared using built-in algorithms of GraphPad Prism 4.03 (GraphPad Software Inc, San Diego, CA). Equimolar comparison was carried out by plotting the points of G protein and  $\beta$ -arr2 BRET dose-response curves for vehicle, -8.0 (only by WIN55), -7.5, -7.0, -6.5, -6.0, -5.5 and -5.0 (only by 2-AG)  $\log$ [WIN55] or  $\log$ [2-AG] (M) treatments of the same receptor against each other. Equiactive comparison was carried out by determining the bias factor ( $\beta$ ) using the equation

$$\beta = \log \left( \left( \frac{E_{\max,1}}{EC_{50,1}} \frac{EC_{50,2}}{E_{\max,2}} \right)_{mut} \times \left( \frac{E_{\max,2}}{EC_{50,2}} \frac{EC_{50,1}}{E_{\max,1}} \right)_{ref} \right), \text{ (Rajagopal et al. 2011), where } E_{\max,1},$$

$EC_{50,1}$ ,  $E_{\max,2}$  and  $EC_{50,2}$  are  $E_{\max}$  and  $EC_{50}$  values from G protein and  $\beta$ -arrestin BRET dose-response curves, respectively, using  $CB_1R$ -WT as reference receptor. Quantified Western-blot data were evaluated with two-way ANOVA combined with Holm-Sidak's post-hoc test, using the software SigmaStat for Windows 3.5 (Systat Software Inc., Richmond, CA), and a p value  $<0.05$  was considered significant.

## 3. Results

### 3.1. Plasma membrane localization of the $CB_1R$ mutants

222

223 To investigate whether any of the mutations inserted into the DRY motif of CB<sub>1</sub>R affects  
224 the proper plasma membrane localization of the receptor, CHO cells expressing mVenus-  
225 tagged CB<sub>1</sub>R variants were analyzed using confocal microscopy. In resting cells, CB<sub>1</sub>R-  
226 mVenus is localized both at the plasma membrane and in intracellular vesicles, consistent  
227 with the constitutive internalization of CB<sub>1</sub>R (Fig. 1A). Importantly, D3.49A mutation  
228 strongly impaired plasma membrane localization of CB<sub>1</sub>R, with most of the receptors  
229 being retained in the endoplasmic reticulum of the cells (CB<sub>1</sub>R-D3.49A-mVenus (CB<sub>1</sub>R-  
230 ARY-mVenus) and CB<sub>1</sub>R-D3.49A/Y3.51A-mVenus (CB<sub>1</sub>R-ARA-mVenus), Fig. 1B and  
231 F, respectively). Interestingly, this effect of the D3.49A mutation was reversed by co-  
232 mutation of R3.50, as the double mutant CB<sub>1</sub>R-D3.49A/R3.50A (CB<sub>1</sub>R-AAY) and the  
233 triple mutant CB<sub>1</sub>R-D3.49A/R3.50A/Y3.51A (CB<sub>1</sub>R-AAA) both showed proper plasma  
234 membrane localization (Fig. 1G and H, respectively). The other three mutants, i.e. CB<sub>1</sub>R-  
235 R3.50A (CB<sub>1</sub>R-DAY), CB<sub>1</sub>R-Y3.51A (CB<sub>1</sub>R-DRA) and CB<sub>1</sub>R-R3.50A/Y3.51A (CB<sub>1</sub>R-  
236 DAA) displayed a cellular distribution roughly similar to that of the wild-type receptor  
237 (Fig 1C, D and E, respectively).

238 Since analysis of confocal images is in many cases not sensitive enough to detect fine  
239 changes in receptor distribution, we also applied a more quantifiable approach here, i.e.  
240 we measured the BRET interaction levels between CB<sub>1</sub>R-mVenus and plasma  
241 membrane-targeted Sluc protein. The fraction of the receptors residing on the plasma  
242 membrane of non-stimulated cells (PM/total receptor BRET) was found to be similar in  
243 cells expressing CB<sub>1</sub>R-WT, CB<sub>1</sub>R-AAY or CB<sub>1</sub>R-AAA, whereas CB<sub>1</sub>R-DAY, CB<sub>1</sub>R-  
244 DRA and CB<sub>1</sub>R-DAA showed an ~40% reduction of plasma membrane localization.

Furthermore, in accordance with confocal images, the plasma membrane localization of CB<sub>1</sub>R-ARY and CB<sub>1</sub>R-ARA was shown to be almost completely diminished (Fig. 1I). Since the plasma membrane localization of the CB<sub>1</sub>R-ARY and CB<sub>1</sub>R-ARA mutants was severely disrupted, these two mutants were not characterized in the subsequent studies.

### *3.2. R3.50A mutation partially affects CB<sub>1</sub>R function*

R3.50 is the most conserved residue within the DRY motif, therefore we first checked the functionality of the CB<sub>1</sub>R-DAY mutant. The G protein activation of the receptor was directly monitored by measuring BRET changes between heterotrimeric G<sub>o</sub> protein subunits ( $\alpha_o$ -Rluc and YFP- $\beta_1\gamma_{11}$ ) (Turu et al. 2007), co-expressed with wild-type or mutant CB<sub>1</sub>R. In control experiments measuring BRET donor and acceptor partner expression directly (i.e. through luminescence and fluorescence counts, respectively) no significant changes were detected between these values when tested with the different CB<sub>1</sub>R mutants, suggesting that the observed changes in BRET were not due to alterations in BRET partner stoichiometry. This applies for all of the G<sub>o</sub> BRET and  $\beta$ -arrestin BRET experiments presented in this study (data not shown). Dose-response curves performed with the synthetic CB<sub>1</sub>R agonist WIN55,212-2 (WIN55) or with the endocannabinoid 2-arachydonoylglycerol (2-AG) showed that the CB<sub>1</sub>R-DAY mutant is impaired, but not completely disrupted in its ability to activate G<sub>o</sub> proteins. Moreover, CB<sub>1</sub>R-DAY shows a basal G protein activation similar to that of CB<sub>1</sub>R-WT (Fig. 2A and B). The EC<sub>50</sub> value of CB<sub>1</sub>R-DAY was also similar to that of CB<sub>1</sub>R-WT, indicating that the G protein binding of CB<sub>1</sub>R is not affected by the R3.50A mutation (Table 1).

268 Next, the  $\beta$ -arr2 recruitment of CB<sub>1</sub>R-DAY was investigated. GFP-tagged  $\beta$ -arr2 ( $\beta$ -arr2-  
269 GFP) was co-expressed with CB<sub>1</sub>R-DAY in CHO cells, and its distribution was analyzed  
270 under confocal microscopy. Interestingly, we found that in cells co-expressing  $\beta$ -arr2-  
271 GFP and CB<sub>1</sub>R-DAY,  $\beta$ -arr2-GFP was recruited to the plasma membrane in punctuate  
272 structures already in resting cells, indicating an increased basal  $\beta$ -arr2 recruitment of  
273 CB<sub>1</sub>R-DAY (Fig. 2E and G). Such basal recruitment of  $\beta$ -arr2-GFP could not be  
274 observed with CB<sub>1</sub>R-WT (Fig. 2C). This basal recruitment of  $\beta$ -arr2 was the  
275 consequence of a partially active receptor conformation, since treatment with the CB<sub>1</sub>R  
276 inverse agonist AM251 (10  $\mu$ M, 10 min) resulted in the disappearance of most of the  $\beta$ -  
277 arr2 puncta from the plasma membrane (Fig. 2H).

278 After addition of the CB<sub>1</sub>R agonist WIN55 (1  $\mu$ M, 10 min) further translocation of  $\beta$ -  
279 arr2-GFP to the plasma membrane could be observed in case of CB<sub>1</sub>R-DAY, however,  
280 this did not reach the level of  $\beta$ -arr2-GFP recruitment of the CB<sub>1</sub>R-WT (Fig. 2D and F).

281 To evaluate  $\beta$ -arr2 recruitment in a more quantitative manner, translocation of  $\beta$ -arr2 to  
282 the receptors was followed by monitoring BRET changes between  $\beta$ -arr2-Rluc and  
283 plasma membrane targeted mVenus (MP-mVenus). With this assay,  $\beta$ -arr2 recruitment to  
284 the investigated receptor can be monitored without tagging the receptor itself directly,  
285 which is advantageous because the detected BRET changes are not influenced by  
286 possible orientational changes resulting from the introduced receptor mutations.

287 Furthermore, BRET signal in this assay is only affected via receptors residing on the  
288 plasma membrane, i.e. BRET ratios are not disturbed by intracellular receptor population.

289 Dose-response curves performed with WIN55 in this  $\beta$ -arr2 BRET assay were in good  
290 accordance with the data obtained by confocal microscopy, i.e. the increased basal  $\beta$ -arr2

recruitment of CB<sub>1</sub>R-DAY, as well as a lower  $\beta$ -arr2 recruitment in response to agonist stimulus were detectable (Fig. 2I). Similar results were obtained with the endocannabinoid 2-AG (Fig. 2J).

### 3.3. Y3.51A mutation increases constitutive activity of CB<sub>1</sub>R

Among the three residues of the DRY motif, Y3.51 is the least conserved, and relatively little is known about its role in 7TMR signaling. To obtain data about its role in CB<sub>1</sub>R regulation, we tested the CB<sub>1</sub>R-DRA mutant under our experimental settings. Interestingly, although the maximal G protein activation of this mutant was only marginally impaired (i.e. a significant change in  $E_{\max}$  was only detectable upon 2-AG stimuli), the G protein BRET dose-response analysis indicated an elevated basal G protein activation for this mutant (Fig. 3A and B, Table 1). Confocal microscopy analysis showed that, similarly to the CB<sub>1</sub>R-DAY mutant, basal  $\beta$ -arr2 recruitment of CB<sub>1</sub>R-DRA occurs (Fig. 3C and E), which could be reversed by inverse agonist treatment (Fig. 3F). Agonist-induced  $\beta$ -arr2-GFP translocation to the plasma membrane was very weak (Fig. 3D).  $\beta$ -arr2 BRET analysis was in accordance with confocal data, namely, dose-response curve showed elevated basal  $\beta$ -arr2 recruitment together with a significantly impaired agonist-induced  $\beta$ -arr2 translocation (Fig. 3G and H).

### 3.4. Enhanced $\beta$ -arrestin2 recruitment and reduced G protein activation of the CB<sub>1</sub>R-*AAV* mutant

Next, we investigated the signaling properties of the double mutant CB<sub>1</sub>R-AAY. The G protein activation was monitored by the BRET assay described above. Dose-response curves carried out with WIN55 or 2-AG showed that the CB<sub>1</sub>R-AAY mutant has impaired G<sub>o</sub> activation ability (Fig. 4A and B), which is reflected both in the E<sub>max</sub> and the pEC<sub>50</sub> values of these interactions (Table 1). Moreover, basal G protein activation of this mutant was significantly lowered ((Fig. 4A and B, Table 1).

The  $\beta$ -arr2 recruitment of CB<sub>1</sub>R-AAY was investigated also by  $\beta$ -arr2-GFP co-expression under confocal microscope. We found that, similarly to CB<sub>1</sub>R-DAY and CB<sub>1</sub>R-DRA, CB<sub>1</sub>R-AAY recruited  $\beta$ -arr2-GFP to the plasma membrane in non-stimulated cells (Fig. 4C and E). The basal  $\beta$ -arr2 recruitment could be reversed with inverse agonist AM251 treatment (Fig. 4F). Upon addition of WIN55, a very robust translocation of  $\beta$ -arr2-GFP to the plasma membrane was observed, with practically no  $\beta$ -arr2-GFP remaining in the cytoplasm (Fig. 4D). We further evaluated the  $\beta$ -arr2 recruitment of CB<sub>1</sub>R-AAY with the BRET-based method described above. WIN55 and 2-AG dose-response curves showed that, in addition to the increased basal  $\beta$ -arr2 recruitment of CB<sub>1</sub>R-AAY, this mutant gained a substantially increased ability to recruit  $\beta$ -arr2 upon agonist stimulus, as shown by the significant left- and upward shift of the curves (Fig. 4G and H, Table 1). These results suggest that the signaling of this mutant is shifted from G protein activation towards  $\beta$ -arr2 recruitment, and therefore CB<sub>1</sub>R-AAY can be considered as a  $\beta$ -arr2-biased mutant.

The characteristics of the triple mutant CB<sub>1</sub>R-AAA) were very similar to that of CB<sub>1</sub>R-AAY, i.e. a decrease in basal and agonist-induced G protein activation, as well as an increase in basal and agonist-induced  $\beta$ -arr2 recruitment were observed (data not shown).

### 3.5. The CB<sub>1</sub>R-DAA mutant is G protein-biased

In the next set of experiments, the functional characteristics of the CB<sub>1</sub>R-DAA double mutant receptor were analyzed. Dose-response curves obtained by G<sub>o</sub> protein BRET assay showed that the CB<sub>1</sub>R-DAA mutant can activate G proteins at a lowered level (~75% of CB<sub>1</sub>R-WT), although pEC<sub>50</sub> values as well as basal G protein activation remained unaffected (Fig. 5A and B, Table 1).

Confocal microscopy analysis of  $\beta$ -arr2-GFP co-expressed with CB<sub>1</sub>R-DAA showed that this mutant, similarly to the CB<sub>1</sub>R-DAY, CB<sub>1</sub>R-DRA and CB<sub>1</sub>R-AAY mutants, recruited  $\beta$ -arr2-GFP to the plasma membrane under control conditions (Fig. 5C and E), and this was reversed by AM251 treatment (Fig. 5F). Interestingly, no further translocation of  $\beta$ -arr2-GFP could be detected in these cells upon addition of the CB<sub>1</sub>R agonist WIN55 (Fig. 5C). These results were strengthened by  $\beta$ -arr2 BRET measurements, showing a basal  $\beta$ -arr2 recruitment for CB<sub>1</sub>R-DAA, which, however, cannot be enhanced by WIN55 or 2-AG treatment (Fig. 5G and H). These results suggest that, in contrast to CB<sub>1</sub>R-AAY, the signaling of CB<sub>1</sub>R-DAA is shifted from  $\beta$ -arr2 recruitment towards G protein activation, and therefore CB<sub>1</sub>R-DAA can be considered as a G protein-biased mutant.

### 3.6. $\beta$ -arrestin1 recruitment of CB<sub>1</sub>R-AAY mutant is robustly enhanced

In our previous study we could not detect significant  $\beta$ -arr1 coupling to the CB<sub>1</sub>R upon WIN55 stimulus, however, others have suggested that CB<sub>1</sub>R dependent  $\beta$ -arr1



recruitment can be present and may regulate ERK1/2 activation of CB<sub>1</sub>R (Laprairie et al., 2014; Flores-Otero et al., 2014). To test whether DRY mutations of CB<sub>1</sub>R affect the recruitment of  $\beta$ -arr1, we applied the same BRET based approach as above, i.e. the plasma membrane translocation of  $\beta$ -arr1-Rluc was monitored, and dose-response curves were performed using WIN55 and 2-AG as agonists. Our results show that agonist-induced  $\beta$ -arr1 recruitment is very low in cells expressing CB<sub>1</sub>R-WT, i.e. a significant increase could only be detected upon 2-AG treatment, whereas the changes obtained with WIN55 proved to be non-significant. Interestingly, the CB<sub>1</sub>R-AAY mutant displayed a robustly enhanced ability to recruit  $\beta$ -arr1, both upon WIN55 and 2-AG stimuli. All of the other three mutants (i.e. CB<sub>1</sub>R-DAY, CB<sub>1</sub>R-DRA and CB<sub>1</sub>R-DAA) produced non-significant changes in the plasma membrane localization of  $\beta$ -arr1 (Fig. 6A and B).

### *3.7. Detailed data analysis strengthens biased signaling of DRY mutant CB<sub>1</sub>Rs*

The above results suggest that distinct mutations in the conserved DRY motif of the CB<sub>1</sub>R can differentially affect G protein activation and  $\beta$ -arr2 recruitment of the receptor. To assess this receptor bias in an exact manner, two different methods, proposed by Rajagopal et al. (Rajagopal et al. 2011), were applied to analyze data. First, ‘equimolar comparison’ was carried out, where G protein and  $\beta$ -arr2 responses elicited by the same ligand concentrations are plotted against each other. In the case of the ‘reference receptor’, i.e. CB<sub>1</sub>R-WT, this analysis yields a roughly hyperbolic shape with both WIN55 and 2-AG (Fig. 7A and B, respectively, black circles), reflecting the difference in the amplification between G protein and  $\beta$ -arr2 assays. Importantly, the points for CB<sub>1</sub>R-

383 AAY are substantially shifted left- and upwards on these graphs, representing bias  
384 towards  $\beta$ -arr2 recruitment (Fig. 7A and B, white triangles). Furthermore, the points for  
385 CB<sub>1</sub>R-DAA are arranged along a horizontal line, demonstrating the bias of this receptor  
386 towards G protein activation (Fig. 7A and B, grey squares). The other method was  
387 ‘equiactive comparison’, where the signaling of each receptor is characterized by a bias  
388 factor ( $\beta$ ), based on the EC<sub>50</sub> and E<sub>max</sub> values from G protein and  $\beta$ -arr2 dose-response  
389 curves (Rajagopal et al. 2011). In case of the reference receptor (CB<sub>1</sub>R-WT), this bias  
390 factor is by definition 0. In the case of CB<sub>1</sub>R-DAA, the  $\beta$  values were 1.42 or 1.61 (for  
391 WIN55 or 2-AG stimuli, respectively), whereas the same values for CB<sub>1</sub>R-AAY were -  
392 1.54 or -1.42, representing more than 10-fold bias of these two mutants towards G protein  
393 activation and  $\beta$ -arr2 recruitment, respectively (Fig. 7C).

394 Taken together, our detailed bias analysis indicated that CB<sub>1</sub>R-AAY and CB<sub>1</sub>R-DAA can  
395 be considered as  $\beta$ -arrestin-biased and G protein-biased mutants, respectively.

### 397 *3.8. Functional assays reflect biased intracellular signaling of CB<sub>1</sub>R-AAY and CB<sub>1</sub>R-* 398 *DAA*

399  
400 Next, we wanted to assess whether the differences seen at the level of receptor-effector  
401 protein coupling are reflected in more distal intracellular signaling events initiated by  
402 CB<sub>1</sub>R activation. First, G<sub>i/o</sub> protein-mediated signaling was assessed by measuring  
403 inhibition of forskolin-induced cAMP accumulation under basal and CB<sub>1</sub>R-stimulated  
404 conditions, using an EPAC-based intramolecular BRET-sensor (Erdelyi et al. 2014). Our  
405 results showed that CB<sub>1</sub>R-WT inhibits cAMP accumulation under non-stimulated

conditions, and this is substantially and dose-dependently enhanced upon treatment with WIN55 (Fig. 8A). Importantly, WIN55-induced cAMP inhibition of the G protein-biased mutant CB<sub>1</sub>R-DAA was lower but still present, whereas CB<sub>1</sub>R-AAY, in accordance with its bias towards  $\beta$ -arr2, failed to induce the inhibition of cAMP accumulation in response to agonist stimulus (Fig. 8A).

Recent data suggest that CB<sub>1</sub>R-induced p42/44 MAP kinase (ERK1/2) activation, which was formerly suggested to occur via G protein-dependent pathways (Galve-Roperh et al. 2002; Davis et al. 2003; Dalton and Howlett 2012), is also mediated by  $\beta$ -arrestins (Ahn et al. 2013a; Mahavadi et al. 2014). Therefore, we aimed to study how the ERK1/2 responses correlate with the G protein activation and/or  $\beta$ -arrestin recruitment of the biased CB<sub>1</sub>R mutants. Western blot experiments carried out with cells expressing CB<sub>1</sub>R-WT showed a robust increase in the amount of phosphorylated ERK1/2 (pERK1/2) after 5 min treatment with WIN55 (1  $\mu$ M). Moreover, lower but sustained pERK1/2 levels were also detectable after 20 min WIN55 treatment (Fig. 7B and C). Interestingly, we found that the  $\beta$ -arr2-biased CB<sub>1</sub>R-AAY elicited pERK1/2 responses similar to CB<sub>1</sub>R-WT, both at 5 and 20 min stimulation, whereas the G protein-biased CB<sub>1</sub>R-DAA produced significantly lower pERK1/2 responses than the wild-type receptor (Fig. 7B and C). Thus, ERK1/2 activation of the biased DRY mutants correlated well with their  $\beta$ -arr2 recruitment ability, rather than with their G protein activation.

#### 4. Discussion

In this study, we evaluated the role of the conserved DRY motif in the function of the CB<sub>1</sub>R. Our goal was to assess its role in mediating basal and agonist-induced G protein activation and  $\beta$ -arrestin recruitment of CB<sub>1</sub>R, as well as to identify possible differences caused in these two main effector functions of the receptor. Interestingly, single alanine mutation of the conserved Arg (R3.50A) resulted only in a ~20% reduction of the G protein coupling efficiency of CB<sub>1</sub>R, without affecting its basal G protein activation. This may seem surprising, as crystal structure analysis as well as several mutational data have suggested a pivotal role for this residue in the G protein coupling of 7TMRs (Zhu et al. 1994; Ballesteros et al. 1998; Rasmussen et al. 2011). However, several other 7TMRs exist, where similar non-conservative mutations of R3.50 failed to abolish G protein activation of the receptor (Fanelli et al. 1999; Rovati et al. 2007). Thus, CB<sub>1</sub>R appears to belong to a subgroup of 7TMRs where this conserved Arg residue plays no absolute role in the direct receptor-G protein coupling. Furthermore, our results demonstrate a basal  $\beta$ -arr2 recruitment of the CB<sub>1</sub>R-DAY mutant (or any double or triple mutant carrying the same mutation), which is in good accordance with previously published data showing similar characteristics for R3.50H mutants of V<sub>2</sub> vasopressin,  $\alpha_{1B}$  adrenergic and AT<sub>1A</sub> angiotensin II receptors (Wilbanks et al. 2002). This strengthens the idea that this conserved Arg somehow prevents arrestin binding in the inactive receptor conformation. Agonist-induced  $\beta$ -arr2 recruitment of CB<sub>1</sub>R-DAY and CB<sub>1</sub>R-DRA was lowered, which is most likely to be caused by the lowered plasma membrane localization of these mutants (Fig. 1I).

The most interesting finding of our study is the major difference between the functions of two double mutants, CB<sub>1</sub>R-DAA and CB<sub>1</sub>R-AAY. Although both mutants contain the

451 R3.50A mutation, and accordingly show increased basal  $\beta$ -arr2 recruitment, their ultimate  
452 characteristics are further determined by the location of the second mutation. Thereby, a  
453 simultaneous lack of D3.49 and R3.50 residues seems to have a dominant-positive effect  
454 on both the  $\beta$ -arr1 and  $\beta$ -arr2 recruitment of CB<sub>1</sub>R (which is also supported by the fact  
455 that the triple mutant CB<sub>1</sub>R-AAA functionally resembles CB<sub>1</sub>R-AAY). Thus, CB<sub>1</sub>R-AAY  
456 is a  $\beta$ -arrestin-biased 7TMR mutant. Interestingly, these characteristics of the CB<sub>1</sub>R-AAY  
457 are similar to those of the formerly described biased mutant angiotensin II receptor AT<sub>1</sub>-  
458 DRY/AAY (AT<sub>1</sub>R-AAY) (Gaborik et al. 2003; Wei et al. 2003). However, an important  
459 difference here is that AT<sub>1</sub>R-AAY is  $\beta$ -arrestin-biased in a way that its G protein  
460 activation is absent while its  $\beta$ -arrestin binding is present but certainly not increased (Wei  
461 et al. 2003, Balla et al., 2012), whereas CB<sub>1</sub>R-AAY is  $\beta$ -arrestin-biased in that its  $\beta$ -  
462 arrestin recruitment is substantially increased, together with a lowered, but not abolished  
463 G protein activating ability. Furthermore, we were able to detect a robustly enhanced  $\beta$ -  
464 arr1 recruitment to CB<sub>1</sub>R-AAY, whereas  $\beta$ -arr1 translocation to CB<sub>1</sub>R-WT was  
465 significant only upon 2-AG stimulus, but not after WIN55 treatment. Thus, it appears that  
466 the recruitment of  $\beta$ -arr1 to CB<sub>1</sub>R-WT is very weak, so that it challenges the limits of  
467 detectability via the (otherwise quite sensitive) BRET approach applied here. However,  
468 our results showing a significant increase of  $\beta$ -arr1 BRET upon 2-AG stimulus are in  
469 accordance with recent results showing higher  $\beta$ -arr1 recruitment by 2-AG compared to  
470 WIN55 (Laprairie et al., 2014). Taken together, recruitment of  $\beta$ -arr1 to CB<sub>1</sub>R-WT is  
471 obviously lower than that of  $\beta$ -arr2, but both are substantially enhanced in the CB<sub>1</sub>R-  
472 AAY mutant. Interestingly, basal G protein activation of CB<sub>1</sub>R-AAY was absent, while  
473 the difference between vehicle-treated and WIN55-stimulated cells remained comparable

474 to that of CB<sub>1</sub>R-WT (Fig. 4A), raising the question whether the reduced E<sub>max</sub> value of  
475 CB<sub>1</sub>R-AAY in this assay reflects a true loss of agonist-induced G protein activation, or it  
476 is caused merely by the absence of basal activity, while WIN55-induced G protein  
477 activation remains unaffected. However, repeating these experiments in HeLa cells,  
478 where basal activity of CB<sub>1</sub>R is minimal (Gyombolai et al. 2013), also showed  
479 substantially impaired WIN55-induced G protein activation of CB<sub>1</sub>R-AAY (Suppl. Fig.  
480 1), suggesting that this mutation reduces not only the basal but also the WIN55-induced  
481 G<sub>o</sub> protein activation of CB<sub>1</sub>R.

482 In contrast, CB<sub>1</sub>R-DAA proved to be G protein-biased, as its  $\beta$ -arrestin recruitment in  
483 response to agonist stimulus was practically absent, but was still able to activate G  
484 proteins, although at a lower level (~70% of the wild type CB<sub>1</sub>R). According to our data,  
485 plasma membrane expression of this mutant is ~40% lower than that of CB<sub>1</sub>R-WT.  
486 However, this extent of decrease is not likely to cause a complete loss of agonist-induced  
487  $\beta$ -arrestin recruitment, given the ~1:1 stoichiometry of receptor- $\beta$ -arrestin complex. This  
488 is also supported by the fact that CB<sub>1</sub>R-DAA still binds  $\beta$ -arr2 under basal conditions.  
489 Other 7TMRs described previously as biased mutants include the M<sub>3</sub>-R3.50L designer  
490 muscarinic receptor (Nakajima and Wess 2012) and  $\beta_2$ -AR-TYY, a triple mutant  $\beta_2$ -AR  
491 which was rationally designed to be functionally selective (Shenoy et al. 2006).  
492 Interestingly, however, all of these mutants are  $\beta$ -arrestin-biased, i.e. they do not couple  
493 to G proteins but still recruit  $\beta$ -arrestin, albeit at a lowered level. The CB<sub>1</sub>R-DAA mutant  
494 presented here is interesting in this respect, as it is biased towards G protein activation,  
495 whereas its mutations affect a 'classical' G protein-coupling region, i.e. the DRY motif.  
496 Intriguingly, although CB<sub>1</sub>R-DAA can hardly recruit  $\beta$ -arrestins in response to agonist

stimulus, it still binds  $\beta$ -arr2 to some extent under non-stimulated conditions. This relies most probably on the presence of the R3.50A mutation, because, as mentioned above, all of the CB<sub>1</sub>R mutants carrying this mutation recruited  $\beta$ -arr2 constitutively. Thus, it seems that the absence of the conserved Arg residue can itself determine a receptor conformation that binds  $\beta$ -arrestin spontaneously. On the other hand, the agonist-induced  $\beta$ -arr2 binding of the receptor can still be strongly influenced in both directions by co-mutations of the neighboring residues.

Taken together, our results obtained with the CB<sub>1</sub>R-AAY and CB<sub>1</sub>R-DAA mutants strongly support a model where the active G protein-coupled and  $\beta$ -arrestin-bound conformations of a 7TMR are different. Moreover, receptor states responsible for constitutive and agonist-induced  $\beta$ -arrestin binding may also show differences.

We also demonstrate here that the agonist-induced ERK1/2 phosphorylation shows good correlation with the  $\beta$ -arr2 recruitment of our biased CB<sub>1</sub>R mutants, rather than their G protein activation or their ability to inhibit forskolin-induced cAMP accumulation. These data are consistent with the recently emerging concept of  $\beta$ -arrestin-dependent CB<sub>1</sub>R signaling, i.e. a  $\beta$ -arrestin-mediated ERK1/2 phosphorylation following CB<sub>1</sub>R activation (Ahn et al. 2013a; Mahavadi et al. 2014).

One of the most interesting questions regarding the DRY mutants presented here is how (i.e. through which molecular structural rearrangements) the distinct mutations induce such large differences in the  $\beta$ -arrestin-recruitment of CB<sub>1</sub>R. One simple explanation would be that mutations of the DRY motif modify primarily the G protein binding of the receptor, and their effects on the  $\beta$ -arr2 recruitment are merely secondary, resulting from the assumption that G proteins and  $\beta$ -arrestins compete for the 7TMR binding. However,

if this would be the only explanation, one should observe an indirect proportionality between the G protein-and the  $\beta$ -arrestin binding abilities of the distinct mutants, which is actually not the case. Thus, mutations of the DRY motif most probably affect  $\beta$ -arr2 binding of CB<sub>1</sub>R independently of its G protein activation. Whether or not the DRY sequence itself is a part of the docking site for arrestins, can not be answered unequivocally based on our results. However, previously published data indicating that the ICL2 loop of 7TMRs, beginning with an intact DRY motif, is part of the  $\beta$ -arrestin binding site, add interesting aspects to our study (Huttenrauch et al. 2002; Marion et al. 2006). Moreover, two recent studies have provided important insights into the structural features within the 7TMR- $\beta$ -arrestin complex. Both of these studies point to an important interaction between the ‘finger loop’ region of  $\beta$ -arrestin and the receptor core, with the direct involvement of the DRY motif (Shukla et al., 2014; Szczepek et al., 2014). Combined with these data, our results show good fit with a model where DRY is directly involved in the  $\beta$ -arrestin binding of CB<sub>1</sub>R. Additionally, mutations of the DRY motif may also affect  $\beta$ -arrestin binding indirectly, i.e. by inducing structural rearrangements in the subsequent ICL2, resulting in diverse, sometimes completely opposite  $\beta$ -arrestin binding phenotypes. However, a more precise understanding of the intramolecular interactions that mediate these characteristics would require the high resolution crystal structure data.

#### **Declaration of interest**

The authors declare no conflict of interest.



## **Funding**

This research was supported by Hungarian Scientific Research Fund (OTKA NK-100883), and a Marie Curie International Outgoing Fellowship within the 7th European Community Framework Programme (PIOF-GA-2009-253628).

## **Author contributions**

P.G. designed and carried out most of the experiments and wrote the manuscript. A.D.T. carried out the  $\beta$ -arr2 BRET experiments, helped with data evaluation and revised the manuscript. D.T. created the CB<sub>1</sub>R-DAY mutant and carried out important control experiments. G.T. created the CB<sub>1</sub>R-AAY mutant, helped with data interpretation and revised the manuscript. L.H. managed the overall project, helped with data interpretation and revised the manuscript.

## **Acknowledgements**

The excellent technical assistance of Ilona Oláh, as well as the help of Bence Szalai with the statistical analyses and presentation of the data is greatly appreciated.

## **References**

Ahn, KH, Mahmoud, MM, Shim, JY & Kendall, DA 2013a Distinct roles of beta-arrestin 1 and beta-arrestin 2 in ORG27569-induced biased signaling and internalization of the cannabinoid receptor 1 (CB1). *The Journal of Biological Chemistry* **288** 9790-9800

566 Ahn, KH, Scott, CE, Abrol, R, Goddard, WA, III & Kendall, DA 2013b  
 567       Computationally-predicted CB1 cannabinoid receptor mutants show distinct  
 568       patterns of salt-bridges that correlate with their level of constitutive activity  
 569       reflected in G protein coupling levels, thermal stability, and ligand binding.  
 570       *Proteins* **81** 1304-1317

571 Azpiazu, I & Gautam, N 2004 A fluorescence resonance energy transfer-based sensor  
 572       indicates that receptor access to a G protein is unrestricted in a living mammalian  
 573       cell. *The Journal of Biological Chemistry* **279** 27709-27718

574 Balla, A, Toth, DJ, Soltesz-Katona, E, Szakadati, G, Erdelyi, LS, Varnai, P & Hunyady,  
 575       L 2012 Mapping of the localization of type 1 angiotensin receptor in membrane  
 576       microdomains using bioluminescence resonance energy transfer-based sensors. *J.*  
 577       *Biol. Chem.* **287** 9090-9099

578 Ballesteros, J, Kitanovic, S, Guarnieri, F, Davies, P, Fromme, BJ, Konvicka, K, Chi, L,  
 579       Millar, RP, Davidson, JS, Weinstein, H & Sealfon, SC 1998 Functional  
 580       microdomains in G-protein-coupled receptors. The conserved arginine-cage motif  
 581       in the gonadotropin-releasing hormone receptor. *The Journal of Biological*  
 582       *Chemistry* **273** 10445-10453

583 Ballesteros, JA, Jensen, AD, Liapakis, G, Rasmussen, SG, Shi, L, Gether, U & Javitch,  
 584       JA 2001 Activation of the beta 2-adrenergic receptor involves disruption of an  
 585       ionic lock between the cytoplasmic ends of transmembrane segments 3 and 6. *The*  
 586       *Journal of Biological Chemistry* **276** 29171-29177

587 Barak, LS, Oakley, RH, Laporte, SA & Caron, MG 2001 Constitutive arrestin-mediated  
588 desensitization of a human vasopressin receptor mutant associated with  
589 nephrogenic diabetes insipidus. *Proceedings of the National Academy of Sciences*  
590 *of the United States of America* **98** 93-98

591 Daigle, TL, Kwok, ML & Mackie, K 2008 Regulation of CB1 cannabinoid receptor  
592 internalization by a promiscuous phosphorylation-dependent mechanism. *Journal*  
593 *of Neurochemistry* **106** 70-82

594 Dalton, GD & Howlett, AC 2012 Cannabinoid CB1 receptors transactivate multiple  
595 receptor tyrosine kinases and regulate serine/threonine kinases to activate ERK in  
596 neuronal cells. *British Journal of Pharmacology* **165** 2497-2511

597 Davis, MI, Ronesi, J & Lovinger, DM 2003 A predominant role for inhibition of the  
598 adenylate cyclase/protein kinase A pathway in ERK activation by cannabinoid  
599 receptor 1 in N1E-115 neuroblastoma cells. *The Journal of Biological Chemistry*  
600 **278** 48973-48980

601 DeWire, SM, Ahn, S, Lefkowitz, RJ & Shenoy, SK 2007 Beta-arrestins and cell  
602 signaling. *Annual Review of Physiology* **69** 483-510

603 Erdelyi, LS, Balla, A, Patocs, A, Toth, M, Varnai, P & Hunyady, L 2014 Altered agonist  
604 sensitivity of a mutant v2 receptor suggests a novel therapeutic strategy for  
605 nephrogenic diabetes insipidus. *Molecular Endocrinology* **28** 634-643

606 Fanelli, F, Barbier, P, Zanchetta, D, de Benedetti, PG & Chini, B 1999 Activation  
 607 mechanism of human oxytocin receptor: a combined study of experimental and  
 608 computer-simulated mutagenesis. *Molecular Pharmacology* **56** 214-225

609 Flores-Otero, J, Ahn, KH, Delgado-Peraza, F, Mackie, K, Kendall, DA & Yudowski, GA  
 610 2014 Ligand-specific endocytic dwell times control functional selectivity of the  
 611 cannabinoid receptor 1. *Nat. Commun.* **5** 4589

612 Gaborik, Z, Jagadeesh, G, Zhang, M, Spat, A, Catt, KJ & Hunyady, L 2003 The role of a  
 613 conserved region of the second intracellular loop in AT1 angiotensin receptor  
 614 activation and signaling. *Endocrinology* **144** 2220-2228

615 Galve-Roperh, I, Rueda, D, Gomez del Pulgar, T, Velasco, G & Guzman, M 2002  
 616 Mechanism of extracellular signal-regulated kinase activation by the CB(1)  
 617 cannabinoid receptor. *Molecular Pharmacology* **62** 1385-1392

618 Glass, M & Northup, JK 1999 Agonist selective regulation of G proteins by cannabinoid  
 619 CB(1) and CB(2) receptors. *Molecular Pharmacology* **56** 1362-1369

620 Gurevich, VV & Benovic, JL 1993 Visual arrestin interaction with rhodopsin. Sequential  
 621 multisite binding ensures strict selectivity toward light-activated phosphorylated  
 622 rhodopsin. *The Journal of Biological Chemistry* **268** 11628-11638

623 Gurevich, VV & Gurevich, EV 2006 The structural basis of arrestin-mediated regulation  
 624 of G-protein-coupled receptors. *Pharmacology & Therapeutics* **110** 465-502

625 Gyombolai, P, Boros, E, Hunyady, L & Turu, G 2013 Differential beta-arrestin2  
626 requirements for constitutive and agonist-induced internalization of the CB1  
627 cannabinoid receptor. *Molecular and Cellular Endocrinology* **372** 116-127

628 Huttenrauch, F, Nitzki, A, Lin, FT, Honing, S & Oppermann, M 2002 Beta-arrestin  
629 binding to CC chemokine receptor 5 requires multiple C-terminal receptor  
630 phosphorylation sites and involves a conserved Asp-Arg-Tyr sequence motif. *The*  
631 *Journal of Biological Chemistry* **277** 30769-30777

632 Kim, KM & Caron, MG 2008 Complementary roles of the DRY motif and C-terminus  
633 tail of GPCRS for G protein coupling and beta-arrestin interaction. *Biochemical*  
634 *and Biophysical Research Communications* **366** 42-47

635 Kouznetsova, M, Kelley, B, Shen, M & Thayer, SA 2002 Desensitization of cannabinoid-  
636 mediated presynaptic inhibition of neurotransmission between rat hippocampal  
637 neurons in culture. *Molecular Pharmacology* **61** 477-485

638 Laprairie, RB, Bagher, AM, Kelly, ME, Dupre, DJ & Denovan-Wright, EM 2014 Type 1  
639 cannabinoid receptor ligands display functional selectivity in a cell culture model  
640 of striatal medium spiny projection neurons. *J. Biol. Chem.* **289** 24845-24862

641 Leterrier, C, Laine, J, Darmon, M, Boudin, H, Rossier, J & Lenkei, Z 2006 Constitutive  
642 activation drives compartment-selective endocytosis and axonal targeting of type  
643 1 cannabinoid receptors. *The Journal of Neuroscience : the Official Journal of the*  
644 *Society for Neuroscience* **26** 3141-3153

645 Li, J, Huang, P, Chen, C, de Riel, JK, Weinstein, H & Liu-Chen, LY 2001 Constitutive  
 646 activation of the mu opioid receptor by mutation of D3.49(164), but not  
 647 D3.32(147): D3.49(164) is critical for stabilization of the inactive form of the  
 648 receptor and for its expression. *Biochemistry* **40** 12039-12050

649 Mahavadi, S, Sriwai, W, Huang, J, Grider, JR & Murthy, KS 2014 Inhibitory signaling  
 650 by CB1 receptors in smooth muscle mediated by GRK5/beta-arrestin activation of  
 651 ERK1/2 and Src kinase. *American Journal of Physiology. Gastrointestinal and*  
 652 *Liver Physiology* **306** G535-G545

653 Marion, S, Oakley, RH, Kim, KM, Caron, MG & Barak, LS 2006 A beta-arrestin binding  
 654 determinant common to the second intracellular loops of rhodopsin family G  
 655 protein-coupled receptors. *The Journal of Biological Chemistry* **281** 2932-2938

656 McDonald, NA, Henstridge, CM, Connolly, CN & Irving, AJ 2007 An essential role for  
 657 constitutive endocytosis, but not activity, in the axonal targeting of the CB1  
 658 cannabinoid receptor. *Molecular Pharmacology* **71** 976-984

659 Mukhopadhyay, S & Howlett, AC 2001 CB1 receptor-G protein association. Subtype  
 660 selectivity is determined by distinct intracellular domains. *European Journal of*  
 661 *Biochemistry / FEBS* **268** 499-505

662 Nakajima, K & Wess, J 2012 Design and functional characterization of a novel, arrestin-  
 663 biased designer G protein-coupled receptor. *Molecular Pharmacology* **82** 575-582

664 Pacher, P, Batkai, S & Kunos, G 2006 The endocannabinoid system as an emerging  
 665 target of pharmacotherapy. *Pharmacological Reviews* **58** 389-462

666 Rajagopal, S, Ahn, S, Rominger, DH, Gowen-MacDonald, W, Lam, CM, DeWire, SM,  
 667 Violin, JD & Lefkowitz, RJ 2011 Quantifying ligand bias at seven-  
 668 transmembrane receptors. *Molecular Pharmacology* **80** 367-377

669 Rasmussen, SG, DeVree, BT, Zou, Y, Kruse, AC, Chung, KY, Kobilka, TS, Thian, FS,  
 670 Chae, PS, Pardon, E, Calinski, D, Mathiesen, JM, Shah, ST, Lyons, JA, Caffrey,  
 671 M, Gellman, SH, Steyaert, J, Skinotitis, G, Weis, WI, Sunahara, RK & Kobilka,  
 672 BK 2011 Crystal structure of the beta2 adrenergic receptor-Gs protein complex.  
 673 *Nature* **477** 549-555

674 Reiter, E, Ahn, S, Shukla, AK & Lefkowitz, RJ 2012 Molecular mechanism of beta-  
 675 arrestin-biased agonism at seven-transmembrane receptors. *Annual Review of*  
 676 *Pharmacology and Toxicology* **52** 179-197

677 Rhee, MH, Nevo, I, Levy, R & Vogel, Z 2000 Role of the highly conserved Asp-Arg-Tyr  
 678 motif in signal transduction of the CB2 cannabinoid receptor. *FEBS Letters* **466**  
 679 300-304

680 Rovati, GE, Capra, V & Neubig, RR 2007 The highly conserved DRY motif of class A G  
 681 protein-coupled receptors: beyond the ground state. *Molecular Pharmacology* **71**  
 682 959-964

683 Scheer, A, Fanelli, F, Costa, T, de Benedetti, PG & Cotecchia, S 1996 Constitutively  
 684 active mutants of the alpha 1B-adrenergic receptor: role of highly conserved polar  
 685 amino acids in receptor activation. *The EMBO Journal* **15** 3566-3578

686 Scheer, A, Fanelli, F, Costa, T, de Benedetti, PG & Cotecchia, S 1997 The activation  
687 process of the alpha1B-adrenergic receptor: potential role of protonation and  
688 hydrophobicity of a highly conserved aspartate. *Proceedings of the National*  
689 *Academy of Sciences of the United States of America* **94** 808-813

690 Scott, CE, Abrol, R, Ahn, KH, Kendall, DA & Goddard, WA, III 2013 Molecular basis  
691 for dramatic changes in cannabinoid CB1 G protein-coupled receptor activation  
692 upon single and double point mutations. *Protein Science : a Publication of the*  
693 *Protein Society* **22** 101-113

694 Shenoy, SK, Drake, MT, Nelson, CD, Houtz, DA, Xiao, K, Madabushi, S, Reiter, E,  
695 Premont, RT, Lichtarge, O & Lefkowitz, RJ 2006 beta-arrestin-dependent, G  
696 protein-independent ERK1/2 activation by the beta2 adrenergic receptor. *The*  
697 *Journal of Biological Chemistry* **281** 1261-1273

698 Shenoy, SK & Lefkowitz, RJ 2011 beta-Arrestin-mediated receptor trafficking and signal  
699 transduction. *Trends in Pharmacological Sciences* **32** 521-533

700 Shim, JY, Ahn, KH & Kendall, DA 2013 Molecular basis of cannabinoid CB1 receptor  
701 coupling to the G protein heterotrimer G $\alpha$ ib $\beta$  $\gamma$ : identification of key  
702 CB1 contacts with the C-terminal helix  $\alpha$ 5 of G $\alpha$ ib $\beta$  $\gamma$ . *The Journal of*  
703 *Biological Chemistry* **288** 32449-32465

704 Shukla, AK, Westfield, GH, Xiao, K, Reis, RI, Huang, LY, Tripathi-Shukla, P, Qian, J,  
705 Li, S, Blanc, A, Oleskie, AN, Dosey, AM, Su, M, Liang, CR, Gu, LL, Shan, JM,  
706 Chen, X, Hanna, R, Choi, M, Yao, XJ, Klink, BU, Kahsai, AW, Sidhu, SS, Koide,



707 S, Penczek, PA, Kossiakoff, AA, Woods, VL, Jr., Kobilka, BK, Skiniotis, G &  
 708 Lefkowitz, RJ 2014 Visualization of arrestin recruitment by a G-protein-coupled  
 709 receptor. *Nature* **512** 218-222

710 Szczepek, M, Beyriere, F, Hofmann, KP, Elgeti, M, Kazmin, R, Rose, A, Bartl, FJ, von  
 711 Stetten, D, Heck, M, Sommer, ME, Hildebrand, PW & Scheerer, P 2014 Crystal  
 712 structure of a common GPCR-binding interface for G protein and arrestin. *Nat.*  
 713 *Commun.* **5** 4801

714 Turu, G & Hunyady, L 2010 Signal transduction of the CB1 cannabinoid receptor.  
 715 *Journal of Molecular Endocrinology* **44** 75-85

716 Turu, G, Simon, A, Gyombolai, P, Szidonya, L, Bagdy, G, Lenkei, Z & Hunyady, L 2007  
 717 The role of diacylglycerol lipase in constitutive and angiotensin AT1 receptor-  
 718 stimulated cannabinoid CB1 receptor activity. *The Journal of Biological*  
 719 *Chemistry* **282** 7753-7757

720 Turu, G, Szidonya, L, Gaborik, Z, Buday, L, Spat, A, Clark, AJ & Hunyady, L 2006  
 721 Differential beta-arrestin binding of AT1 and AT2 angiotensin receptors. *FEBS*  
 722 *Letters* **580** 41-45

723 Varnai, P, Toth, B, Toth, DJ, Hunyady, L & Balla, T 2007 Visualization and  
 724 manipulation of plasma membrane-endoplasmic reticulum contact sites indicates  
 725 the presence of additional molecular components within the STIM1-Orai1  
 726 Complex. *The Journal of Biological Chemistry* **282** 29678-29690

727 Venkatakrishnan, AJ, Deupi, X, Lebon, G, Tate, CG, Schertler, GF & Babu, MM 2013  
728 Molecular signatures of G-protein-coupled receptors. *Nature* **494** 185-194

729 Wei, H, Ahn, S, Shenoy, SK, Karnik, SS, Hunyady, L, Luttrell, LM & Lefkowitz, RJ  
730 2003 Independent beta-arrestin 2 and G protein-mediated pathways for  
731 angiotensin II activation of extracellular signal-regulated kinases 1 and 2.  
732 *Proceedings of the National Academy of Sciences of the United States of America*  
733 **100** 10782-10787

734 Wilbanks, AM, Laporte, SA, Bohn, LM, Barak, LS & Caron, MG 2002 Apparent loss-of-  
735 function mutant GPCRs revealed as constitutively desensitized receptors.  
736 *Biochemistry* **41** 11981-11989

737 Woo, J & von Arnim, AG 2008 Mutational optimization of the coelenterazine-dependent  
738 luciferase from Renilla. *Plant Methods* **4** 23

739 Zhu, SZ, Wang, SZ, Hu, J & el Fakahany, EE 1994 An arginine residue conserved in  
740 most G protein-coupled receptors is essential for the function of the m1  
741 muscarinic receptor. *Molecular Pharmacology* **45** 517-523

742

743

744

## Figure legends

### **Fig.1 Cellular distribution of wild-type and mutant mVenus-tagged CB<sub>1</sub>R variants**

A-H, CHO cells expressing mVenus-tagged CB<sub>1</sub>R variants are visualized using confocal microscopy. A, CB<sub>1</sub>R-WT-mVenus B, CB<sub>1</sub>R-ARY-mVenus C, CB<sub>1</sub>R-DAY-mVenus, D, CB<sub>1</sub>R-DRA-mVenus E, CB<sub>1</sub>R-DAA-mVenus F, CB<sub>1</sub>R-ARA-mVenus G, CB<sub>1</sub>R-AAY-mVenus H, CB<sub>1</sub>R-AAA-mVenus. Images are representative from 3 independent experiments. Scale bar 10  $\mu$ m. I, PM/total receptor BRET showing the fraction of mVenus-tagged CB<sub>1</sub>R variants residing on the plasma membrane. 0% reflects no net BRET interaction and 100% reflects normalized BRET interaction of CB<sub>1</sub>R-WT-mVenus. Data are mean $\pm$ SEM, n=3, \*p<0.05, ns – non-significant

### **Fig.2 Functional analysis of the CB<sub>1</sub>R-DAY mutant**

A-B, Dose-response curves showing G protein activation of CB<sub>1</sub>R-WT (grey curve) and CB<sub>1</sub>R-DAY (black curve) in CHO cells under basal and different WIN55- (A) or 2-AG- (B) stimulated conditions, as detected by G<sub>o</sub> protein BRET. 0% reflects total inactivity of receptors, achieved by inverse agonist treatment (AM251, 10  $\mu$ M), and 100% reflects maximal WIN55- (A) or 2-AG- (B) induced response ( $E_{max}$ ) of CB<sub>1</sub>R-WT. Data are mean $\pm$ SEM, n=3-8.

C-H, Confocal images showing distribution of  $\beta$ -arr2-GFP in CHO cells co-expressing CB<sub>1</sub>R-WT (C and D) or CB<sub>1</sub>R-DAY (E-H), under control conditions (C, E and G) and 10 min after WIN55 (1  $\mu$ M, D and F) or AM251 (10  $\mu$ M, H) treatment. Arrows indicate  $\beta$ -

arr2-GFP puncta at the plasma membrane. Images are representative from at least 4 independent experiments. Scale bar 10  $\mu$ m.

I-J, Dose-response curves showing recruitment of  $\beta$ -arr2 to the plasma membrane by CB<sub>1</sub>R-WT (grey curve) and CB<sub>1</sub>R-DAY (black curve) in CHO cells under basal and different WIN55- (I) or 2-AG- (J) stimulated conditions, as detected by BRET between  $\beta$ -arr2-Rluc and MP-mVenus. 0% reflects total inactivity of receptors, achieved by inverse agonist treatment (AM251, 10  $\mu$ M), and 100% reflects maximal WIN55- (I) or 2-AG- (J) induced response ( $E_{\max}$ ) of CB<sub>1</sub>R-WT. Data are mean $\pm$ SEM, n=4-7.

### **Fig.3 Functional analysis of the CB<sub>1</sub>R-DRA mutant**

A-B, Dose-response curves showing G protein activation of CB<sub>1</sub>R-WT (grey curve) and CB<sub>1</sub>R-DRA (black curve) in CHO cells under basal and different WIN55- (A) or 2-AG- (B) stimulated conditions, as detected by G<sub>o</sub> protein BRET. 0% reflects total inactivity of receptors, achieved by inverse agonist treatment (AM251, 10  $\mu$ M), and 100% reflects maximal WIN55- (A) or 2-AG- (B) induced response ( $E_{\max}$ ) of CB<sub>1</sub>R-WT. Data are mean $\pm$ SEM, n=4-8.

C-F, Confocal images showing distribution of  $\beta$ -arr2-GFP in CHO cells co-expressing CB<sub>1</sub>R-DRA, under control conditions (C and E) and 10 min after WIN55 (1  $\mu$ M, D) or AM251 (10  $\mu$ M, F) treatment. Arrows indicate  $\beta$ -arr2-GFP puncta at the plasma membrane. Images are representative from at least 4 independent experiments. Scale bar 10  $\mu$ m.

G-H, Dose-response curves showing recruitment of  $\beta$ -arr2 to the plasma membrane by CB<sub>1</sub>R-WT (grey curve) and CB<sub>1</sub>R-DRA (black curve) in CHO cells under basal and

different WIN55- (G) or 2-AG- (H) stimulated conditions, as detected by BRET between  $\beta$ -arr2-Rluc and MP-mVenus. 0% reflects total inactivity of receptors, achieved by inverse agonist treatment (AM251, 10  $\mu$ M), and 100% reflects maximal WIN55- (G) or 2-AG- (H) induced response ( $E_{\max}$ ) of CB<sub>1</sub>R-WT. Data are mean $\pm$ SEM, n=4-7.

**Fig.4 Functional analysis of the CB<sub>1</sub>R-AAV mutant**

A-B, Dose-response curves showing G protein activation of CB<sub>1</sub>R-WT (grey curve) and CB<sub>1</sub>R-AAV (black curve) in CHO cells under basal and different WIN55- (A) or 2-AG- (B) stimulated conditions, as detected by G<sub>o</sub> protein BRET. 0% reflects total inactivity of receptors, achieved by inverse agonist treatment (AM251, 10  $\mu$ M), and 100% reflects maximal WIN55- (A) or 2-AG- (B) induced response ( $E_{\max}$ ) of CB<sub>1</sub>R-WT. Data are mean $\pm$ SEM, n=3-8.

C-F, Confocal images showing distribution of  $\beta$ -arr2-GFP in CHO cells co-expressing CB<sub>1</sub>R-AAV, under control conditions (C and E) and 10 min after WIN55 (1  $\mu$ M, D) or AM251 (10  $\mu$ M, F) treatment. Images are representative from at least 3 independent experiments. Scale bar 10  $\mu$ m.

G-H, Dose-response curves showing recruitment of  $\beta$ -arr2 to the plasma membrane by CB<sub>1</sub>R-WT (grey curve) and CB<sub>1</sub>R-AAV (black curve) in CHO cells under basal and different WIN55- (G) or 2-AG- (H) stimulated conditions, as detected by BRET between  $\beta$ -arr2-Rluc and MP-mVenus. 0% reflects total inactivity of receptors, achieved by inverse agonist treatment (AM251, 10  $\mu$ M), and 100% reflects maximal WIN55- (G) or 2-AG- (H) induced response ( $E_{\max}$ ) of CB<sub>1</sub>R-WT. Data are mean $\pm$ SEM, n=4-7.

**Fig.5 Functional analysis of the CB<sub>1</sub>R-DAA mutant**

A-B, Dose-response curves showing G protein activation of CB<sub>1</sub>R-WT (grey curve) and CB<sub>1</sub>R-DAA (black curve) in CHO cells under basal and different WIN55- (A) or 2-AG- (B) stimulated conditions, as detected by G<sub>o</sub> protein BRET. 0% reflects total inactivity of receptors, achieved by inverse agonist treatment (AM251, 10  $\mu$ M), and 100% reflects maximal WIN55- (A) or 2-AG- (B) induced response ( $E_{\max}$ ) of CB<sub>1</sub>R-WT. Data are mean $\pm$ SEM, n=4-8.

C-F, Confocal images showing distribution of  $\beta$ -arr2-GFP in CHO cells co-expressing CB<sub>1</sub>R-DAA, under control conditions (C and E) and 10 min after WIN55 (1  $\mu$ M, D) or AM251 (10  $\mu$ M, F) treatment. Images are representative from at least 3 independent experiments. Scale bar 10  $\mu$ m.

G-H, Dose-response curves showing recruitment of  $\beta$ -arr2 to the plasma membrane by CB<sub>1</sub>R-WT (grey curve) and CB<sub>1</sub>R-DAA (black triangles) in CHO cells under basal and different WIN55- (G) or 2-AG- (H) stimulated conditions, as detected by BRET between  $\beta$ -arr2-Rluc and MP-mVenus. 0% reflects total inactivity of receptors, achieved by inverse agonist treatment (AM251, 10  $\mu$ M), and 100% reflects maximal WIN55- (G) or 2-AG- (H) induced response ( $E_{\max}$ ) of CB<sub>1</sub>R-WT. Data are mean $\pm$ SEM, n=4-7.

**Fig.6 Dose-response curves showing  $\beta$ -arrestin1 recruitment of CB<sub>1</sub>R mutants**

A-B, Dose-response curves showing recruitment of  $\beta$ -arr1 to the plasma membrane by CB<sub>1</sub>R-WT (black circles), CB<sub>1</sub>R-DAY (white diamonds), CB<sub>1</sub>R-DRA (white circles), CB<sub>1</sub>R-DAA (white squares) or CB<sub>1</sub>R-AAY (white triangles) in CHO cells under basal and different WIN55- (A) or 2-AG- (B) stimulated conditions, as detected by BRET

between  $\beta$ -arr1-Rluc and MP-mVenus. 0% reflects total inactivity of receptors, achieved by inverse agonist treatment (AM251, 10  $\mu$ M), and 100% reflects maximal WIN55- (A) or 2-AG- (B) induced response ( $E_{\max}$ ) of CB<sub>1</sub>R-AAV. Data are mean $\pm$ SEM, n=3. \*p<0.05 vs vehicle treatment.

#### **Fig.7 Bias analysis showing functional selectivity of CB<sub>1</sub>R mutants**

A-B, Equimolar comparison of CB<sub>1</sub>R-WT (black points), CB<sub>1</sub>R-DAA (grey squares) and CB<sub>1</sub>R-AAV (white triangles) functions. For each receptor, responses from G protein and  $\beta$ -arr2 BRET dose-response curves, elicited by the same WIN55 (A) or 2-AG (B) concentration, were plotted against each other. The left- and upward shift of CB<sub>1</sub>R-AAV points represents bias toward  $\beta$ -arr2 recruitment, whereas the downward shift of CB<sub>1</sub>R-DAA points indicates G protein bias. Data are mean $\pm$ SEM. C, Equiactive comparison of CB<sub>1</sub>R-WT, CB<sub>1</sub>R-DAA and CB<sub>1</sub>R-AAV functions. The biased factor ( $\beta$ ) was calculated for each receptor, based upon  $EC_{50}$  and  $E_{\max}$  values of G protein and  $\beta$ -arr2 BRET dose-response curves obtained with WIN55 (black bars) or 2-AG (grey bars) stimuli, using the equation described in *Materials and methods*. CB<sub>1</sub>R-WT was used as reference receptor. Positive values indicate bias towards G protein signaling, whereas negative values reflect  $\beta$ -arrestin bias. Data are mean  $\pm$  SD.

#### **Fig.8 Functional assays measuring intracellular signaling of wild-type and mutant CB<sub>1</sub>R variants**

A, Dose-response curves showing the inhibition of forskolin-induced cAMP accumulation in CHO cells expressing CB<sub>1</sub>R-WT, CB<sub>1</sub>R-DAA or CB<sub>1</sub>R-AAV under

basal and different WIN55-stimulated conditions, measured by the BRET changes of an EPAC-based intramolecular BRET sensor. BRET was measured 30 min after stimulus. 0% reflects total inactivity of receptors, achieved by inverse agonist treatment (AM251, 10  $\mu$ M), and 100% reflects maximal WIN55-induced response ( $E_{\max}$ ) of CB<sub>1</sub>R-WT. Data are mean $\pm$ SEM, n=6. \*p<0.05 vs basal state, #p<0.05 vs CB<sub>1</sub>R-WT. B, Amounts of phosphorylated (pERK1/2) and total ERK1/2 proteins detected by Western blot in CHO cells expressing CB<sub>1</sub>R-WT, CB<sub>1</sub>R-DAA or CB<sub>1</sub>R-AAY, after 0, 5 or 20 min of WIN55 (1  $\mu$ M) treatment. Images are representative from four independent experiments. C, Quantification of Western blot data. 0% reflects background intensity, and 100% reflects WIN55-induced pERK1/2 intensity of CB<sub>1</sub>R-WT at 5 min. Data are mean $\pm$ SEM, n=4, \*p<0.05 versus CB<sub>1</sub>R-WT at 5 min, #p<0.05 versus CB<sub>1</sub>R-WT at 20 min.

#### **Supplementary Fig. 1 G protein activation of CB<sub>1</sub>R-AAY mutant in HeLa cells**

BRET measurements showing G<sub>o</sub> protein activation of CB<sub>1</sub>R-WT and CB<sub>1</sub>R-AAY in HeLa cells under basal (white bars) and WIN55-stimulated (1  $\mu$ M, black bars) conditions. 0% reflects total inactivity of receptors, achieved by inverse agonist treatment (AM251, 10  $\mu$ M), and 100% reflects WIN55-induced response of CB<sub>1</sub>R-WT. Data are mean $\pm$ SEM, n=4. \*p<0.05 vs basal, #p<0.05 vs CB<sub>1</sub>R-WT.

#### **Table 1. Parameters of G<sub>o</sub> BRET and $\beta$ -arrestin2 BRET dose-response curves for the different CB<sub>1</sub>R variants**

Bottom and  $E_{\max}$  values are expressed as % of  $E_{\max}$  of CB<sub>1</sub>R-WT. Data are mean $\pm$ SEM, n=3-8. \*p<0.05 vs CB<sub>1</sub>R-WT. n.d. – not detectable

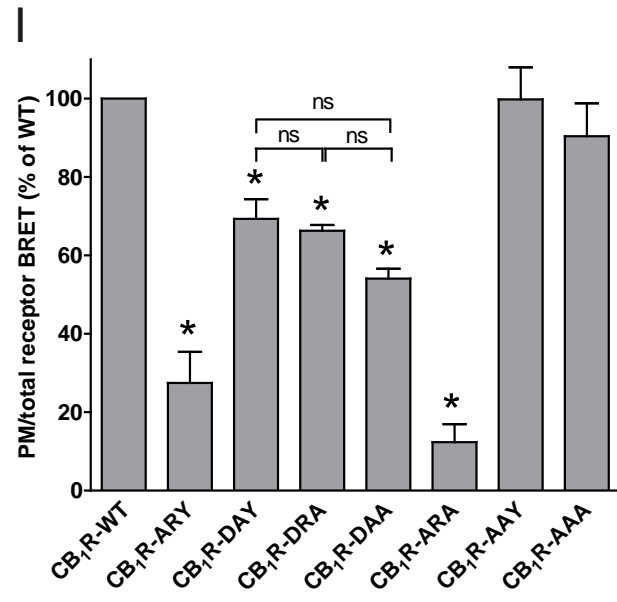
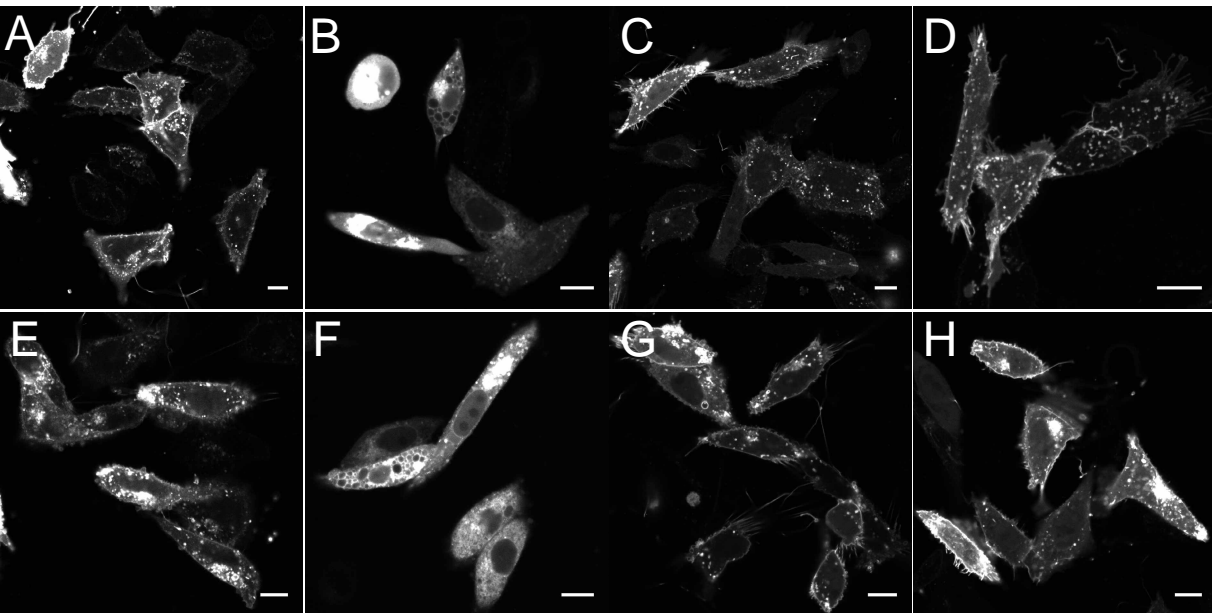


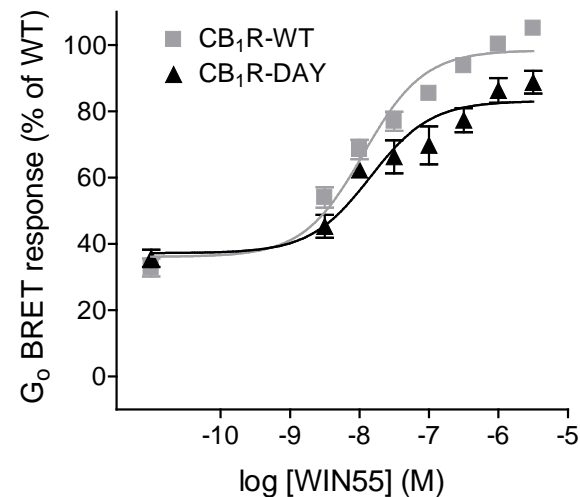
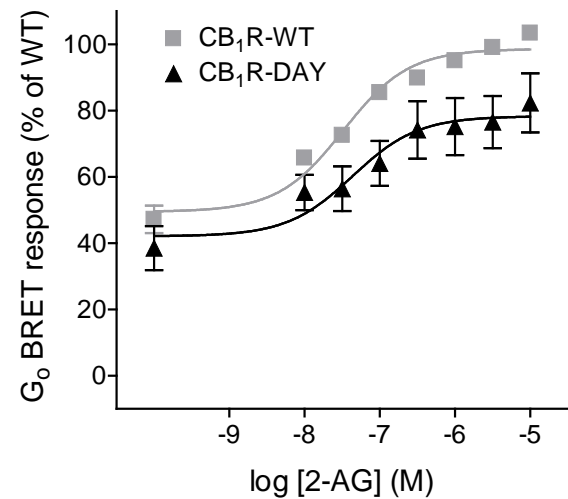
882

883

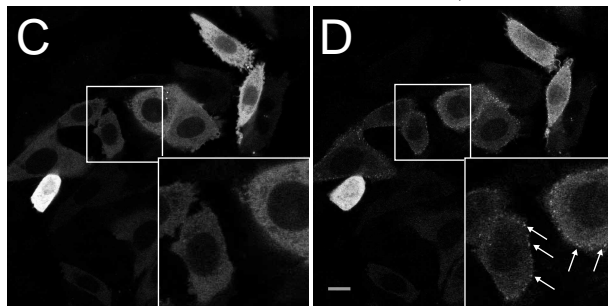
884

Figure 1

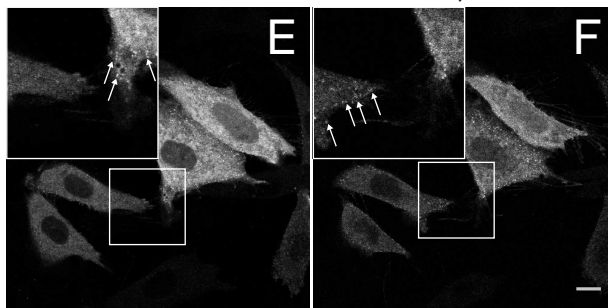


**Figure 2****A****B**

$\beta$ -arr2-GFP + CB<sub>1</sub>R-WT  
control WIN55, 10 min



$\beta$ -arr2-GFP + CB<sub>1</sub>R-DAY  
control WIN55, 10 min



control, cell bottom AM251, 10 min

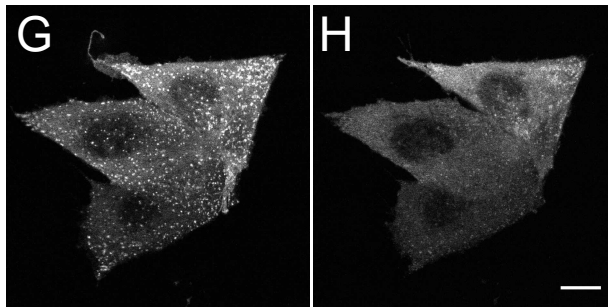
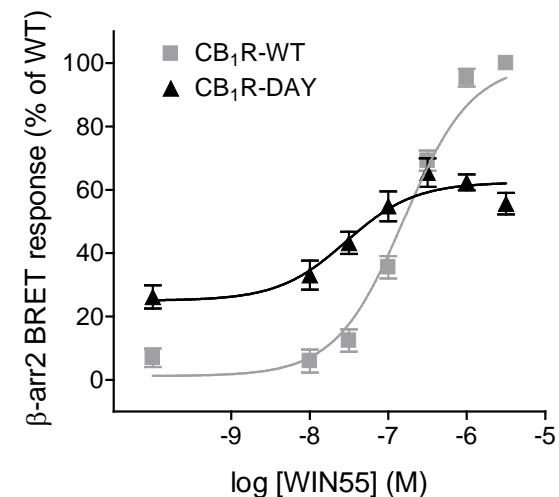
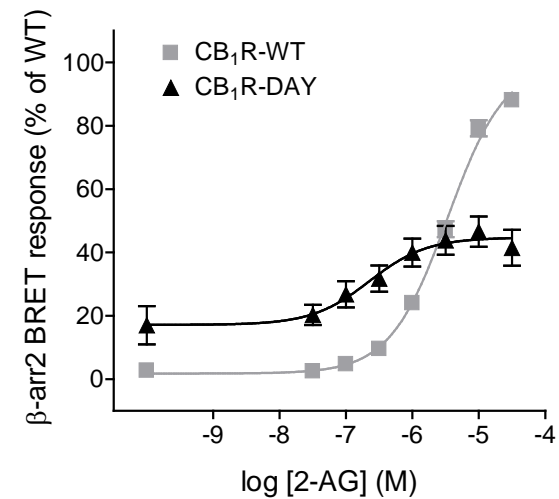
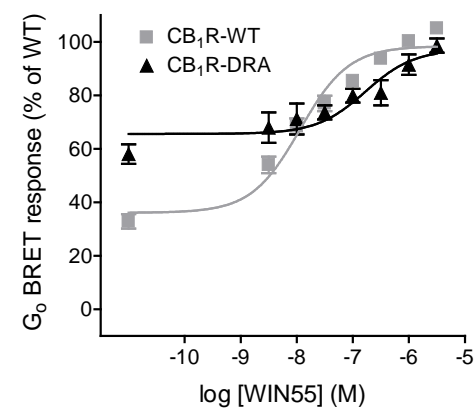
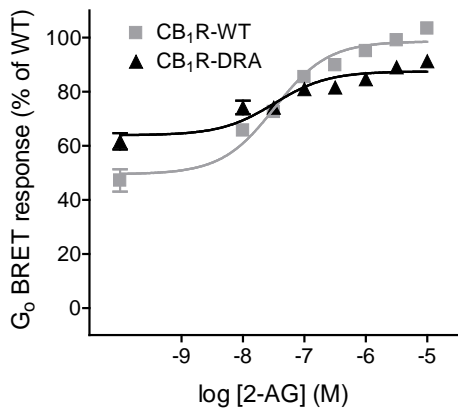
**I****J**

Figure 3

A



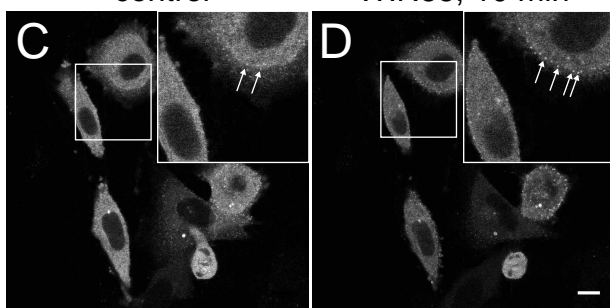
B



$\beta$ -arr2-GFP + CB<sub>1</sub>R-DRA

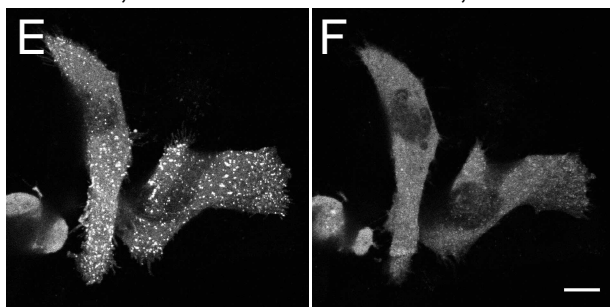
control

WIN55, 10 min

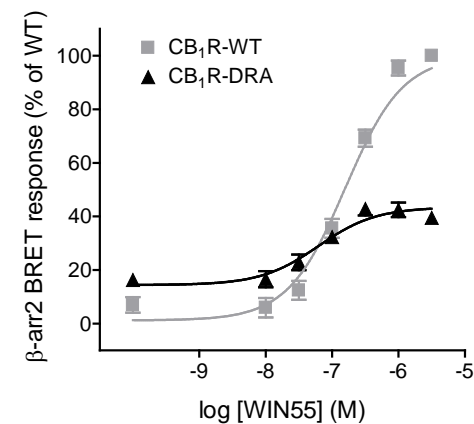


control, cell bottom

AM251, 10 min



G



H

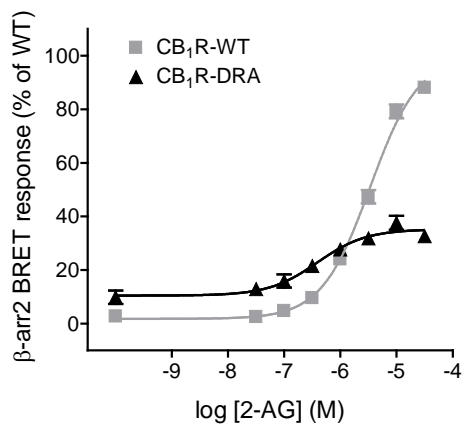


Figure 4

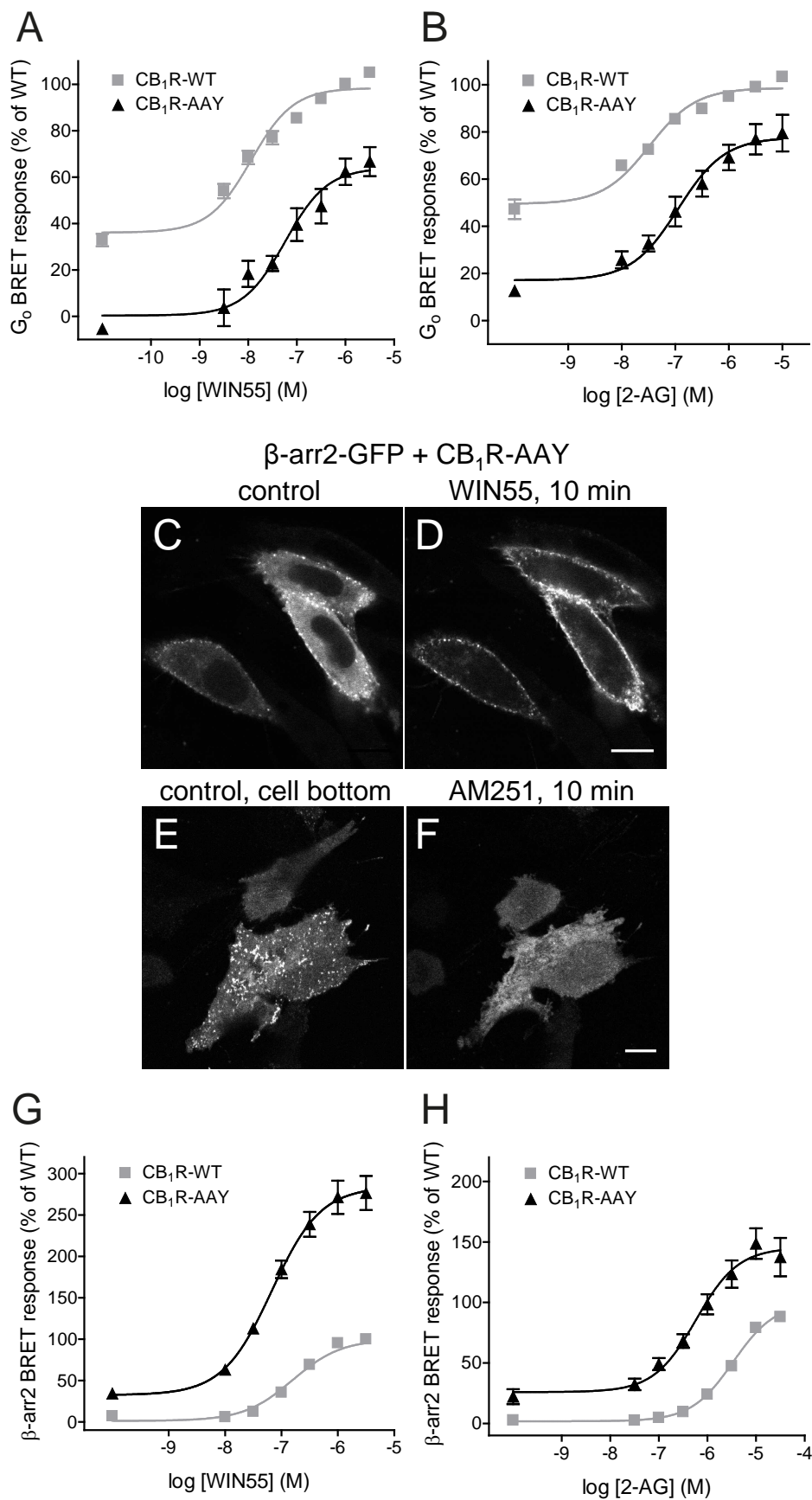


Figure 5

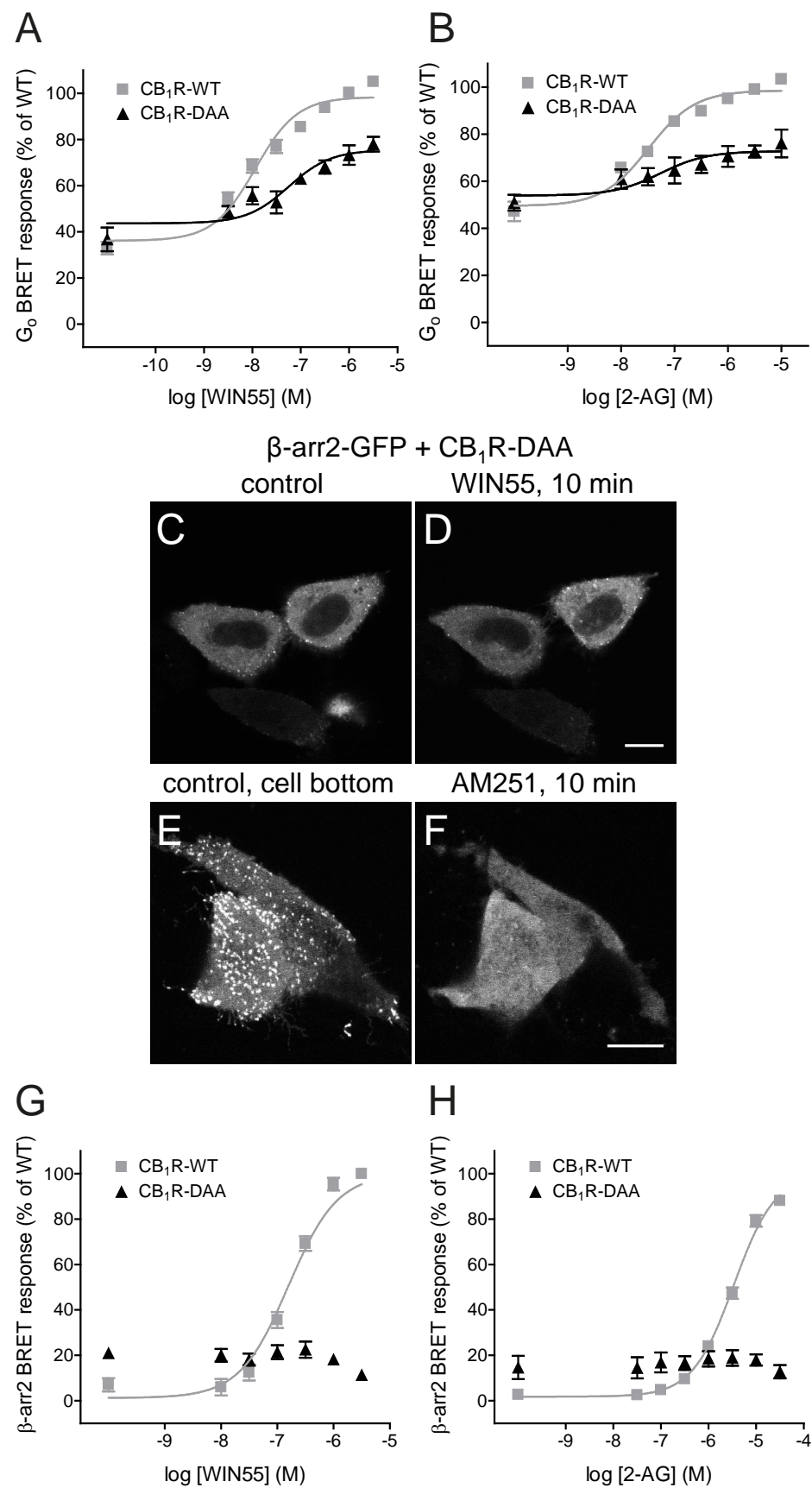
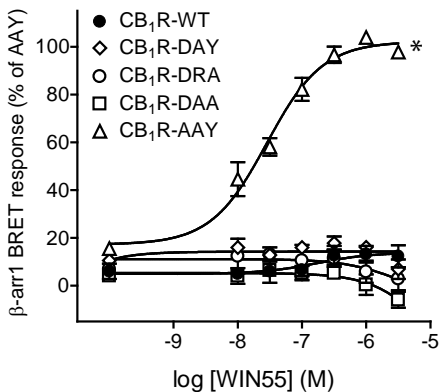
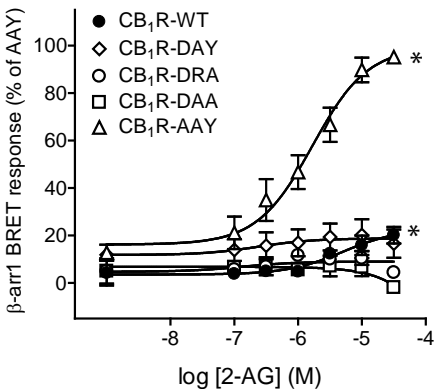


Figure 6

A

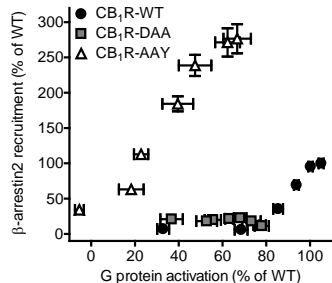


B

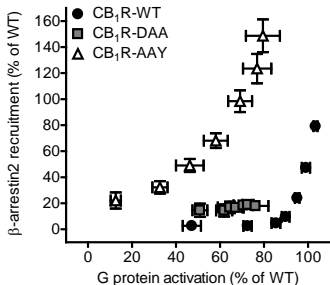


# Figure 7

## A



## B



## C

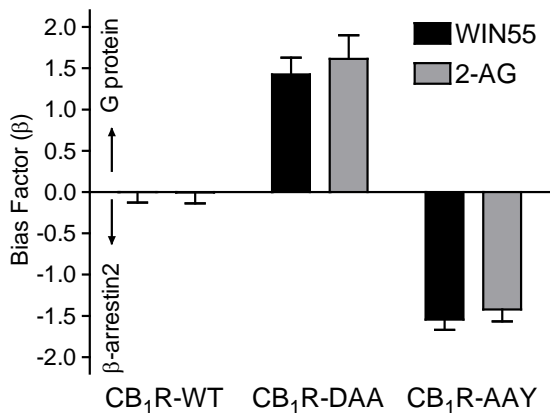
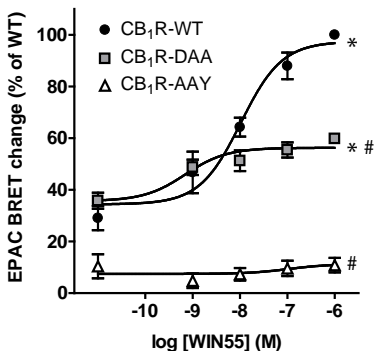


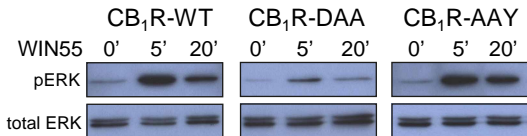


# Figure 8

## A



## B



## C

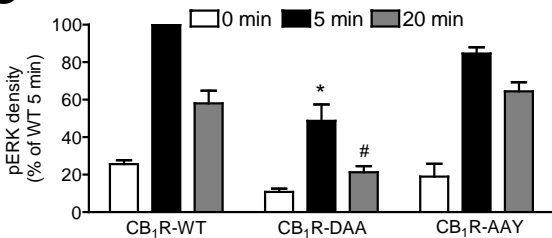


**Table 1**

| G <sub>o</sub> BRET   |                   |             |                  |                   |             |                  |
|-----------------------|-------------------|-------------|------------------|-------------------|-------------|------------------|
| WIN55                 |                   |             |                  | 2-AG              |             |                  |
| Receptor              | pEC <sub>50</sub> | bottom      | E <sub>max</sub> | pEC <sub>50</sub> | bottom      | E <sub>max</sub> |
| CB <sub>1</sub> R-WT  | -7.89±0.07        | 36.85±2.47  | 100              | -7.43±0.07        | 50.11±2.18  | 100              |
| CB <sub>1</sub> R-DAY | -7.85±0.17        | 37.19±3.95  | 83.12±3.95*      | -7.36±0.34        | 42.11±6.35  | 78.31±4.10*      |
| CB <sub>1</sub> R-DRA | -6.78±0.27*       | 65.58±2.62* | 97.22±4.31       | -7.49±0.18        | 63.90±2.28* | 87.49±1.35*      |
| CB <sub>1</sub> R-DAA | -7.25±0.23        | 43.62±2.86  | 75.45±2.92*      | -7.26±0.39        | 53.99±3.56  | 72.79±2.48*      |
| CB <sub>1</sub> R-AAY | -7.24±0.17*       | 0.36±4.24*  | 64.06±4.43*      | -6.95±0.15*       | 17.12±4.02* | 77.69±3.52*      |

| β-arr2 BRET           |                   |              |                  |                   |             |                  |
|-----------------------|-------------------|--------------|------------------|-------------------|-------------|------------------|
| WIN55                 |                   |              |                  | 2-AG              |             |                  |
| Receptor              | pEC <sub>50</sub> | bottom       | E <sub>max</sub> | pEC <sub>50</sub> | bottom      | E <sub>max</sub> |
| CB <sub>1</sub> R-WT  | -6.80±0.051       | 1.23±2.53    | 100              | -5.47±0.02        | 1.79±0.87   | 100              |
| CB <sub>1</sub> R-DAY | -7.53±0.19*       | 25.13±3.77*  | 62.36±2.60*      | -6.65±0.28*       | 17.15±3.64* | 44.72±2.71*      |
| CB <sub>1</sub> R-DRA | -7.21±0.16*       | 14.43±2.09*  | 43.46±1.84*      | -6.41±0.16*       | 10.47±1.69* | 35.22±1.52*      |
| CB <sub>1</sub> R-DAA | > -5.0*           | 20.96±2.35*  | n.d.             | > -4.5*           | 14.62±5.10* | n.d.             |
| CB <sub>1</sub> R-AAY | -7.17±0.10*       | 32.68±10.90* | 284.10±9.93*     | -6.24±0.14*       | 25.91±6.44* | 145.30±6.74*     |

# Supplementary Figure 1

